A First Numerical Simulation of the Development and Structure of the Sea Breeze in the Island of Mallorca

C. Ramis R. Romero

Geophysical Fluid Dynamics Group, Departament de Fisica, Universitat de les Illes Balears, Palma de Mallorca, Spain

Ann. Geophy., **13**, 981-994 (1995)

Corresponding author address: Dr. Clemente Ramis, Dept. de Fisica, Universitat de les Illes Balears, 07071 Palma de Mallorca, Spain
E-mail: cramis@uib.es

Abstract

A numerical study of the development and structure of the sea breeze in Mallorca is presented using a meso-β numerical model. The model includes a detailed representation of the soil and vegetation processes. The study covers a diurnal cycle. The results show that the model reproduces the main known features of the circulation and new ones appear which seem to have appreciable effect on the circulation during the decay of the sea breeze. The orography and the soil dryness have been identified as the main factors determining the structure of the breeze. Three more experiments have been performed in order to isolate the effect of each factor.

1 Introduction

The atmospheric circulation developed by differential heating between land and water is among the most studied mesoscale atmospheric circulations (Atkinson 1981). There are descriptive and observational studies of the sea breeze at many places around the world and in particular for some coasts in the Mediterranean Sea (Neumann, 1951; Bitan, 1981; Lalas et al., 1983 ; Prezerakos, 1986 among others). Other studies have put the emphasis on the fine structure of the planetary boundary layer (PBL) associated with such circulation (Druilhet et al., 1982; Helmis et al., 1987). Since the differential heating sources are geographically fixed, this kind of mesoscale circulation has been numerically simulated much more frequently than the circulations forced by dynamical instabilities. So mesoscale numerical models have simulated the sea breeze structure at fixed locations (e.g. Carpenter, 1979; Mahfouf et al., 1987b) or have been applied, in theoretical and simple cases, to study the effects of topography on the sea and land breezes (Mahrer and Pielke, 1977; Asai and Mitsumoto, 1978; Ookuchi et al., 1978).

The introduction of soil and vegetation effects in mesoscale numerical models has improved the accuracy of such models. Recent studies have emphasized the important role played by soil texture through its influence on surface moisture availability. They have indicated that for soils with adequate water supply, dense vegetation cover becomes the dominant surface factor in the evolution of the PBL but soil properties must be taken into account in cases of sparse vegetation or when the soil is subjected to a water deficit (Pinty et al., 1989). With those conditions, thermally induced circulations associated with differential heating between zones of different soil or vegetation properties have been simulated (e. g. Mahfouf et al., 1987a).

The development of these mesoscale models allows to carry out numerical simulations of real cases of sea-land thermally induced circulations including cases in which the effects of the orography can be decisive on its structure. In this sense, this paper presents numerical experiments carried out using a three-dimensional meso-β model, with a detailed representation of the soil-atmosphere interface, of the breeze circulation in the island of

Mallorca.

The paper contains a description of the breeze in the island and meteorological conditions in which it develops (section 2). Section 3 includes a brief description of the model used to perform the numerical experiments. Section 4 contains an explanation of the atmospheric initial conditions and soil properties. Results are presented in section 5. A study about the influence of orography and soil dryness on the structure of the breeze is included in section 6. Finally, section 7 contains conclusions.

2 Sea breeze in Mallorca

The island of Mallorca is located in the centre of the Western Mediterranean (between 39^0 and 40^0 N and 2.5^0 and 3.5^0 E). It measures 100 x 80 km^2 approximately and possesses three major relief units: the high relief of the Serra de Tramontana in the west and northwest, with the highest point of 1440 m at Puig Major; a central lowland plateau; and the eastern uplands of the Serra de Llevant, reaching up to 500 m above sea level. Two big bays are situated in the northeast and the southwest (see Fig. 1). The coast is smooth except in the northwest where there are sharp cliffs. A long beach occurs along the south coast of the island.

The meteorological conditions during the summer over the Western Mediterranean are normally very favourable for the development of the breeze circulation. In fact, the synoptic scale over this area is dominated by the Azores anticyclone which even extends its influence to central Europe. As a consequence of the thermal low-pressure developed over the Iberian peninsula, the anticyclonic circulation, and therefore the stability, become reinforced over the Western Mediterranean (Fig. 2) favouring sunshine and fair weather.

Another favourable condition to produce the thermal differential heating is that the total heat flux from the surface over land results displaced toward the sensible heat in detriment of the latent heat. In fact, most of the island of Mallorca is very dry during summer and the soil water deficit is present after the beginning of June. As an example, Fig. 3 represents the Thornthwaite hydric balance in Llucmajor, a town on the south of the island (see Fig. 1), and shows that the water deficit exceeds 140 mm in July.

These climatological features result in the development of the sea breeze in Mallorca, often from April to October and almost every day during July and August. In fact at the airport, close to the bay of Palma (see Fig. 1), the frequency of the apparition of the sea breeze at 1200 UTC is 80% of the days in July and 76% in August. In spite of this high frequency, there are only a few studies about it: Jansà and Jaume (1946) published a paper showing some details from an inquiry made among farmers and fishermen. Ramis and Alonso (1988) showed a satellite observation of the clouds formed by the circulation and Ramis et al. (1990) presented a numerical simulation using a very simple one-level model.

Figure 4, from Jansà and Jaume (1946), shows the main features of the sea breeze in its mature state. The main structure is the convergence line, located in the centre of the island, and formed by the flux from the two bays. Other convergence zones can be identified, specially in the northeast and the west. On the northwest side of the island the mountain range blocks the current. This scheme also shows that the eastern slope of that mountain range could participate in the final structure of the full developed circulation as a consequence of the slope winds generated in the morning.

3 The model

The model used to perform the simulations is an hydrostatic three-dimensional meso-β model developed by Nickerson et al. (1986). The Coriolis force is included. Model equations are expressed in a terrain-following coordinates system, where the vertical coordinate ν is related to the usual sigma coordinate by the expression

$$\sigma = (4\nu - \nu^4)/3$$

The ν coordinate has the advantage of allowing for a high resolution of the PBL in spite of working with an uniform grid.

The horizontal diffusion is introduced by a fourth-order operator and the exchange coefficients for the vertical turbulent mixing are calculated as functions of the turbulent kinetic energy (TKE) following Therry and Lacarrère (1983) and Bougeault and Lacarrère

(1989).

The energy and water budget equations are solved at the air-soil interface to obtain the temperature and moisture at the surface. As explained in Mahfouf et al. (1987) and Pinty et al. (1989), vertical diffusion equations for temperature and volumetric water content are solved in the multi-layer soil following McCumber and Pielke (1981). Based on Deardorff (1978), the surface scheme also allows the inclusion of a single layer of vegetation which is assumed to have negligible heat capacity. A second energy budget is established for the foliage layer taking into account the exchanges above and below the canopy. Calculations of solar and infrared fluxes are based on Mahrer and Pielke (1977).

4 Initial conditions and surface parameters

In the experiment shown the astronomical parameters for radiation correspond to 15 July at a latitude of 40^0N. The simulation begins at 0500 LST (due to the location of Mallorca the local time practically matches UTC) and covers the diurnal cycle. The model domain is 150 x 150 km^2 with an horizontal grid length of 2.5 km.

4.1 The atmosphere

We have used 30 vertical levels resulting in 9 computational levels in the lowest kilometer, the first of which is approximately 4.5 meters above the ground. A high resolution of the PBL is very convenient in this kind of simulations.

The model has been initialized with a single radiosounding, providing horizontally uniform fields at the beginning of the simulation. This radiosounding (Fig. 5) corresponds to the mean vertical structure of the atmosphere over Mallorca for July at 0000 UTC (Ramis 1976). The wind is initially calm. During the simulation, all the fields are relaxed toward their initial values at the lateral boundaries (Davies, 1976).

4.2 The surface

In spite of its small size, the island of Mallorca presents a complex distribution of vegetative covers and soil textures. This aspect could influence the structure of the breeze through the spatial and temporal distribution of surface fluxes and friction. For that reason, a detailed representation of vegetation covers and soil characteristics has been considered.

Figures 6a and 6b show the distribution of soil and vegetation types on the island used for the simulation. The maps are a coarse version of soil and vegetation charts of the region. Landsat images have been considered in addition to the charts information. Five representative textural classes and vegetative covers have been considered. The characteristic parameters required by the surface submodel have been approximated based on previous classifications (Tables 1 and 2). Areas of sparse vegetation are mixed with others of dense cover as can be seen in Fig. 6c, which shows the shielding factor.

The sea surface temperature is 25^0C. The initial temperature on the land surface corresponds to the distribution of the mean minimum temperature during July over the island.

The soil, supposed to have a depth of 1 m, is divided into 13 vertical levels. Subsurface measurements are not available at present. As a consequence, temperature and moisture profiles have been initialized in a simple way. The temperature profile is initially homogeneous, given by the value at the soil surface. Representing the soil state during summer, which presents a strong water deficit (see Fig. 3), the volumetric water content (see Table 3) is given as a function of the soil type but is very low at the surface and increases a little with the depth (Vadell, personal communication). However, the listed values are modified by a regional multiplicative factor in order to account for the heterogeneous mean pluviometry on the island. The spatial distribution of the multiplicative factor is shown in Fig. 6d.

5 Results and discussion

5.1 Model results

As was indicated previously, a simulation for a diurnal cycle has been run. The wind distribution at different times over the island corresponding to the lowest level of the model (4.5 m above the ground) are presented in Fig. 7.

At 0900 LST (Fig. 7a) the breeze penetrates inland only a few kilometers except in the northwest coast where the wind is very weak. The breeze front is easily identified. The flux is stronger from the bay of Palma. The influence of the eastern slope of the Serra de Tramontana can be identified: the flux from the two bays is veering and backing, respectively, toward that warmer slope.

The circulation becomes developed after 1200 LST with a clear appearance of the convergence line in the centre of the island. Fig. 7b shows the wind distribution at 1500 LST and represents the fully developed state. It may be compared with Fig. 4a. The convergence line formed between the breezes from the two bays is represented as well as other smaller convergence zones in the northeast, close to the coast, in the southeast as a continuation of the main convergence and over the eastern part of the main range mountain, in good correspondence with Fig. 4b. Two small and very shallow cyclonic circulations have appeared in the simulation at this time. The first one in the centre of the island is a consequence of the shear between the main fluxes and the heat flux from the soil to the air. This cyclonic circulation can be considered as a small thermal low since its thermal structure, as we will show later, is similar, in a smaller scale, to that previously identified in such kinds of systems. The second is located over the west of the island, in the south of a notable mountain group. Much more than a lee development, it may be considered as a result of a cape effect combined with the fact that the breeze is a shallow circulation.

The simulation shows that the breeze weakens very quickly after 1900 LST. At 2100 LST (Fig. 7c) a weak cyclonic circulation remains around the island. However the small cyclones seem to maintain still their influence on the breeze. In fact, that previously located in the centre has moved to the north and influences the wind in the northern part of the island. At the same time, the cyclonic circulation previously located over the west has moved to the east, being over the coast of the bay of Palma and dominates the circulation in the bay and south coasts.

The structure at the end of the simulated diurnal cycle (0500 LST) is presented in Fig. 7d. Although some remaining winds can be appreciated to the north and southwest of the island, the circulation is very weak. A slight land breeze has developed at the same time over the coast of the south, east and northeast. A simulation for a second diurnal cycle shows that the circulation appears again with similar timing and characteristics.

The vertical structure of the circulation has been studied by means of cross sections along the lines AB, which includes the strongest winds at low levels, and CD, which includes the convergence line (see Fig. 1).

The Fig. 8a shows the vertical structure of the wind component along AB at 1500 LST. This section shows that the sea breeze, when fully developed, has a depth smaller than 1 km. The maximum winds occur over the coast but the wind from the bay of Alcudia reaches higher values. The convergence in the centre of the island is very strong with large values for the acceleration of the currents. The counter-current has also a depth of approximately 1 km but with values lesser than for the current. The greater values of the counter-current are from the northeast and located over the bay of Palma. The cross section along the convergence line CD (Fig. 8b) shows that in this direction the sea breeze is shallower than along the AB direction. In the northwest of the island the breeze does not overcome the mountain range and becomes restricted over the sea, whereas on the eastern coast the wind can overcome the mountains, although with smaller speeds with respect to the other direction. Although some evidence of convergence can be appreciated over the eastern part of the island, the central part of the section is entirely dominated by divergence in contrast with section AB, where convergence at low levels corresponds to divergence at upper levels.

The vertical velocity at 1500 LST along the cross section AB is shown in Fig. 9. As a consequence of the convergence over the centre of the island, a region of strong and concentrated upward vertical motion is developed, with velocity values that exceed 35 $\mathrm{cm\,s^{-1}}$. A secondary zone of upward velocity is produced by the southwest flux due to orographic lifting. The descending motion is very slow and spread with values that do not exceed 10 $\mathrm{cm\,s^{-1}}$.

The perturbation on the temperature field at 1500 LST along AB as a consequence of the solar radiation is presented in Fig. 10. The perturbation is limited to the lowest 3 km but the most important feature occurs at low levels where the isentropes intercept the surface, determining a dome of superadiabatic lapse rate and therefore of absolute instability. The higher temperatures are reached in the centre of the island where the small cyclone appears. This thermal configuration, associated with the circulation, resembles, at a smaller scale, that observed over the Iberian peninsula when thermal low pressure develops during the summer (Alonso et al., 1994).

5.2 Verification of results

The model results have been compared against observations made at different points over the island during July 1993, in particular with the data from four automatic weather stations, the aeronautical observations in the airport and the data from a climatic observatory (see Fig. 1 for location). In all the observatories, there are for different days, some differences in the breeze data as a consequence of the influence on the local circulation of the particular synoptic situation. For this reason the model results must be considered as an approximation to the mean aspects of the breeze, since the initialization process uses horizontally uniform atmospheric mean values and does not include background flux.

Figure 11 shows the comparison between the temporal sequence given by the model and observations at the automatic weather station AS1 (see Fig. 1 for location). The wind direction (Fig. 11a) matches very well with the observations including the change observed about 2000 LST. In the model, this change is produced by the displacement of the cyclonic circulation developed on the west side of the island toward the coast of the bay of Palma. This result supports the development of such small circulation and explains the observed change in the wind direction. Figure 11b shows that the model overestimates the wind speed, especially during the central hours of the day, but also shows that it represents well the decrease and posterior increase of the wind speed associated with the change in the wind direction. Despite the initialization of the atmospheric fields based on the mean sounding of July, and the crude initial soil profiles, the tendencies for the temperature and relative humidity given by the model close to the surface are again in agreement with those indicated by the observations (Figs. 11c and 11d).

Figure 12 displays the model results and observations in AS2. Wind speed and direction are well represented by the model except between 1400 and 1600 LST. During this interval the observed wind direction changes between northwest and northeast despite the previous and posterior dominant direction being south-southwest. At the same time the wind speed decreases but afterwards increases to recover the tendency previously indicated. This abnormal structure at this particular day can be due to the local formation, south to the position given by the model, of the central cyclonic circulation. This is the only evidence of such development since this anomalous change is not observed on other days in AS2 and the model reproduces well the wind data.

The model underestimates the wind speed in AS3 as can be seen in Fig. 13b, but reproduces well the direction (Fig. 13a), especially during the afternoon. This underestimation is observed during the majority of the days selected for verification.

The agreement between observed data and model results is quite good in AS4 (Fig. 14). A particular feature that appears in AS4 is that the wind maintains an appreciable value during the evening in contrast with the other stations where the wind decreases rapidily to very small values after 2100 LST. The model reproduces this behaviour in AS4.

The comparison between the aeronautical observations in the airport (A in Fig. 1) and the model results (Fig. 15) shows that the simulation is good in direction as well as in the speed of the wind. Although the climatological observations in C (see Fig. 1) are limited to three values during the day, the model results match well with the data at these particular times.

6 Influence of the orography and soil dryness on the breeze circulation

Following Stein and Alpert (1993), to isolate the effect of n factors by means of numerical simulations, it is necessary to perform 2^n simulations. From the previous results and other simulations made with different conditions for the soil, it seems that the main factors which determine the structure of the sea breeze in Mallorca are the orography and the soil dryness. So, three more experiments have been made in order to isolate the effects of these two factors. Table 4 shows the characteristics of the whole set of experiments.

We identify as f_0 the experiment without orography and with saturated soil, f_1 represents the experiment with orography and saturated soil, f_2 without orography and with dry soil (which characteristics were described in section 4.2) and f_{12} is the complete experiment with orography and dry soil, already discussed in section 5. Except for these two factors the rest of parameters are initially the same for the four experiments. The contributions associated with both factors are determinated by

1. Effect of the orography $\quad f_1^* = f_1 - f_0$
2. Effect of the soil dryness $\quad f_2^* = f_2 - f_0$
3. Effect of the interaction orography - soil dryness $\quad f_{12}^* = f_{12} - (f_1 + f_2) + f_0$

Results for experiments f_0, f_1 and f_2 at 1500 LST are shown in Fig. 16. For experiment f_0, the absence of orography supposes that the breeze developed along the northwest coast can progress inland. In the rest of the island, the wind field is similar to the complete case, but the circulation is weaker and not fully developed, in such way that the convergence line does not appear (Fig. 16a). When the orography is included (experiment f_1), the structure is very similar to the complete case but the circulation and the convergence in the centre of the island are weaker. Moreover, the central cyclone is not identified (Fig. 16b). Experiment f_2 shows that with dry soil and flat terrain, the breeze developed along the northwestern coast is able to progress much further inland than in experiment f_0 and to arrive at the Bay of Palma. In the same manner, the flux from the eastern coast can reach the Bay of Alcudia. The strongest fluxes are again those developed along the coasts of the main bays. The central cyclone is well marked in this experiment (Fig. 16c).

Figure 17 shows the effects on the mature breeze of each factor and the effect due to the interaction between orography and dryness. The action of the orography is presented in Fig. 17a. This action is very strong over the east slope of the Serra de Tramontana. The presence of the strongest f_1^* winds towards the coast in this area shows that the block by the Serra de Tramontana on the sea breeze along the northwest coast is decisive to define the full structure of the circulation. From a direct examination of the results f_1 and f_0 (Figs. 16b and 16a respectively), we can deduce that the veering of the breeze toward the main range is also due to the orography by the heating of the eastern slope. Although to a lesser extent, the Serra de Llevant is also blocking the breeze from the eastern coast. The blocking action from both relief units can even be observed over the sea along the corresponding coast lines, since the f_1^* winds are outward from the island. Another important effect of the orography is the development of the cyclonic circulation over the west of the island. This structure is absolutely separated by the orographic factor. Moreover, another cyclonic circulation appears over the Bay of Alcudia. The contribution of the orography to the development of the cyclonic circulation in the centre of the island seems to be very weak.

Figure 17b shows the effect of the soil dryness. The main effect is to increase the wind over practically all the island and to permit the fluxes from the two bays to form the convergence line in the centre. The cyclonic circulation in the centre becomes completely determined by this factor, which does not participate in the other cyclonic circulation that appears in the full structure. Curiously, close to the Bay of Palma the dryness effect f_2^* seems to be in opposition to the development of the breeze. This behaviour is associated, as we noted previously, with the fact that the breeze developed without orography along the northwestern coast is able to arrive at the Bay of Palma when the soil is dry but not when the soil is wet.

The effect of the interaction between dryness and orography is presented in Fig. 17c. This contribution seems to work to compensate for the dryness effect. In fact, its action is strong over the same areas where the dryness acts appreciably, but is directed in the opposite sense. The strongest f_{12}^{*} winds are found again inland near the Bay of Palma. This fact could be associated with an enhancement of the slope winds, which are favoured in this area due to the shape and dimensions of the south basin (see Fig. 1).

7 Conclusions

The results show the ability of the mesoscale models to reproduce sea breeze circulations on small islands like Mallorca, where the orography is complex and becomes fundamental in the full structure of the circulation.

The general structure and diurnal cycle are well reproduced by the model and show general aspects developed by theoretical studies.

The convergence zones are well located as well as the blocking action by the principal mountain range. Some small and new structures have appeared in the model results: a small and shallow cyclonic circulation in the centre and another one over the west of the island. These systems move from their genesis areas during the process of the decay of the sea breeze and become important in the remaining circulation.

The model shows that the island has enough size to develop, in a small scale, a thermal structure similar to that observed in greater systems produced by heating, as for example the thermal low over the Iberian peninsula.

The orography and soil dryness, identified as the principal factors of the structure and development of the sea breeze, seem to play an important role. The Serra de Tramontana is high enough to block the current along the northwest coast, but at the same time develops a slope wind circulation on its eastern slope which is decisive in the full circulation. The orography is also responsible of the development of the west cyclonic circulation by the cape effect. The main action of the dryness over the circulation is to enhance the wind over all the coasts, except close to the bay of Palma, in such a way that the convergence line in the centre of the island does not occur when the soil is wet. The interaction between orography and dryness acts in the opposite direction to the dryness contribution, enhancing the slope winds in the south basin.

The presented simulation of the full case, entirely produced by differential heating forcing, matches well with observations, but must be considered as a first aproximation due to the fact that the actual breeze can be enhanced, reduced or modified by the synoptic flux. Simulations with different synoptic fluxes can help to know their action on the main features of the breeze. However, the results presented in this work probably represent the best known, at the moment, about the breeze in the island of Mallorca, and can help for others studies such as environmental applications, or serve as a guide to potential users such as sailors.

Acknowledgements. The authors gratefully acknowledge the assistance of the Meteorological Centre of Palma de Mallorca for providing the observational data used in this work. The authors also thank J. Vadell (Department of Environmental Biology, UIB) for his help in the determination of the surface characteristics of Mallorca. This work has been partially supported by DGICYT PB89-0428 grant.

REFERENCES

Alonso, S., A. Portela and C. Ramis, First considerations on the structure and development of the Iberian thermal low-pressure system, *Ann. Geophy.,* **12,** 457-468, 1994.

Asai, T. and S. Mitsumoto, Effects of an inclined land surface on the land and sea breeze circulation. A numerical experiment, *J. Meteor. Soc. Japan,* **56,** 559-570, 1978.

Atkinson, B. W., *Mesoscale Atmospheric Circulations,* Academic Press, New York, 495pp, 1981.

Bitan, A., Lake Kinneret (Sea of Galilea) and its exceptional wind system, *Bound. Layer Meteor.,* **21,** 477-487, 1981.

Bougeault, P. and P. Lacarrère, Parameterization of orographic induced turbulence in a mesobeta scale model, *Mon. Wea. Rev.,* **117,** 1872-1890, 1989.

Carpenter, K. M., An experimental forecast using a nonhydrostatic model, *Quart. J. Roy. Meteor. Soc.,* **105,** 629-655, 1979.

Clapp, R., and G. Hornberger, Empirical equations for some soil hydraulic properties, *Water Resour. Res.*, **14,** 601-604, 1978.

Davies, H. C., A lateral boundary formulation for multilevel prediction models, *Quart. J. R. Meteor. Soc.,* **102,** 405-418, 1976.

Deardorff, J. W., Efficient prediction of ground surface temperature and moisture, with inclusion of a layer of vegetation, *J. Geoph. Res.,* **83,** 1889-1903, 1978.

Druilhet, A., A. Herrada, J.P. Pages, J. Sassai, C. Allet and M. Ravaut, Etude expérimentale de la couche limite interne associée à la brise de mer, *Bound. Layer*

Meteor., **22,** 511-524, 1982.

Font, I., *Climatología de España y Portugal,* Instituto Nacional de Meteorología, Madrid, 1983.

Helmis, C. G., D. N. Asimakopoulos, D. G. Deligiorgi and D. P. Lalas, Observations of sea breeze fronts near the shoreline, *Bound. Layer Meteor.,* **38,** 395-410, 1987.

Jansà, J. M. and E. Jaume, The sea breeze regime in the Mallorca island (in spanish), *Rev. de Geofísica,* **19,** 304-328, 1946.

Lalas, D. P., D. N. Asimakopoulos, D. G. Deligiorgi and C. G. Helmis, Sea-breeze circulation and photochemical pollution in Athens, Greece, *Atmos. Environ.,* **17,** 1621-1632, 1983.

Mahfouf, J. F., E. Richard and P. Mascart, The influence of soil and vegetation on the development of mesoscale circulations, *J. Climate Appl. Meteor.,* **26,** 1483-1495, 1987a.

Mahfouf, J. F., E. Richard, P. Mascart, E. C. Nickerson and R. Rosset, A comparative study of various parameterizations of the Planetary Boundary Layer in a numerical mesoscale model, *J. Climate Appl. Meteor.,* **26,** 1671-1695, 1987b.

Mahrer, Y. and R. A. Pielke, The effects of topography on the sea and land breezes in a two-dimensional numerical model, *Mon. Wea. Rev.,* **105,** 1151-1162, 1977.

McCumber, M. C., *A numerical simulation of the influence of heat and moisture fluxes upon mesoscale circulations,* Ph. D. dissertation, University of Virginia, 255 pp, 1980.

McCumber, M. C. and R. A. Pielke, Simulation of the effects of surface fluxes of heat and moisture in a mesoscale numerical model. 1. Soil layer, *J. Geoph. Res.,* **86,** 9929-9938, 1981.

Neumann, J., Land breezes and nocturnal thunderstorms, *J. Meteor.,* **8,** 60-67, 1951.

Nickerson, E. C., E. Richard, R. Rosset and D. R. Smith, The numerical simulation of clouds, rain and airflow over the Vosges and Black forest mountain: a meso-β model with parameterized microphysics, *Mon. Wea. Rev.,* **114,** 398-414, 1986.

Ookouchi, Y., M. Uryu and R. Sawada, A numerical study of the effects of a mountain on the land and sea breezes, *J. Meteor. Soc. Japan,* **56,** 368-385, 1978.

Pinty, J. P., P. Mascart, E. Richard and R. Rosset, An investigation of mesoscale flows induced by vegetation inhomogeneities using an evapotranspiration model calibrated against HAPEX-MOBILHY data, *J. Appl. Meteor.,* **28,** 976-992, 1989.

Prezerakos, N. G., Characteristics of the sea breeze in Attica, Greece, *Bound. Layer Meteor.,* **36,** 245-266, 1986.

Ramis, C., *Climatology of the upper air over Mallorca (in spanish),* Univ. de Barcelona, 66 pp., 1976.

Ramis, C. and S. Alonso, Sea breeze convergence line in Mallorca. A satellite observation, *Weather,* **43,** 288-293, 1988.

Ramis, C., A. Jansà and S. Alonso, Sea breeze in Mallorca. A numerical study, *Meteorol. Atmos. Phys.,* **42,** 249-258, 1990.

Stein, U. and P. Alpert, Factor separation in numerical simulations, *J. Atm. Sci.,* **50,** 2107-2115, 1993.

Therry, G. and P. Lacarrère, Improving the eddy-kinetic energy model for planetary boundary layer description, *Bound. Layer Meteor.,* **25,** 63-88, 1983.

Soil type	η_s	K_{η_s} (.10^{-6} m s^{-1})	ψ_s (m)	$\rho_i c_i$ (.10^6 J m^{-3} K^{-1})	b	ε	a	z_0 (mm)
Sand	0.395	176.0	-0.121	1.463	4.05	0.99	0.25	5
Sandy Loam	0.410	156.0	-0.090	1.404	4.38	0.99	0.25	5
Silt Loam	0.430	25.0	-0.200	1.300	4.80	0.99	0.30	5
Clay Loam	0.460	3.0	-0.440	1.150	8.40	0.99	0.25	5
Clay	0.482	1.3	-0.405	1.089	11.40	0.99	0.35	5

Table 1: Soil parameters for five textural classes representative of Mallorca. The parameters have been computed combining those given in the classification of the U. S. Department of Agriculture (Clapp and Hornberger, 1978; McCumber, 1980): η_s (soil porosity), K_{η_s} (saturated hydraulic conductivity), ψ_s (saturated moisture potential), $\rho_i c_i$ (dry volumetric heat capacity) and b (dimensionless exponent). ε is the emissivity, a the albedo and z_0 the roughness length.

	Vegetation type				
Parameter	**Tall Grass**	**Shrub**	**Crop**	**Conifer Forest**	**Woodland**
Height (m)	2.0	0.5	0.4	12.0	10.0
Displacement height (m)	1.50	0.37	0.30	9.00	7.50
Plant resistance (s)	8.10^9	10.10^9	6.10^9	8.10^9	8.10^9
Minimum stomatal resistance (s m^{-1})	350	500	50	350	350
Critical leaf water potential (m)	-150	-150	-100	-150	-180
Green leaf area index	2.0	1.0	1.0	3.5	5.0
Dry leaf area index	2.0	2.0	0.1	0.7	1.0
Canopy emissivity	0.98	0.98	0.96	0.98	0.98
Canopy albedo	0.16	0.16	0.20	0.10	0.15
Roughness length (m)	0.17	0.04	0.03	1.00	0.83
Average rooting depth (m)	0.2	0.2	0.2	0.9	0.9

Table 2: Parameters of five representative types of vegetation of Mallorca. The values have been approximated using the HAPEX-MOBILHY data (Pinty et al., 1988).

Soil type	η_{up}	η_{down}
Sand	0.005	0.020
Sandy Loam	0.020	0.060
Silt Loam	0.030	0.090
Clay Loam	0.040	0.100
Clay	0.050	0.110

Table 3: Representative volumetric water content as a function of soil type for the case of Mallorca during July. η_{up} corresponds to the upper 10 cm layer and η_{down} to the 90 cm layer below.

Experiment	Orography	Soil Dryness
f_0	NO	NO
f_1	YES	NO
f_2	NO	YES
f_{12}	YES	YES

Table 4: Summary of the numerical experiments performed in order to isolate the effect of the orography and soil dryness on the breeze circulation over Mallorca. f_{12} is the complete or actual case commented in section 5.

FIGURES

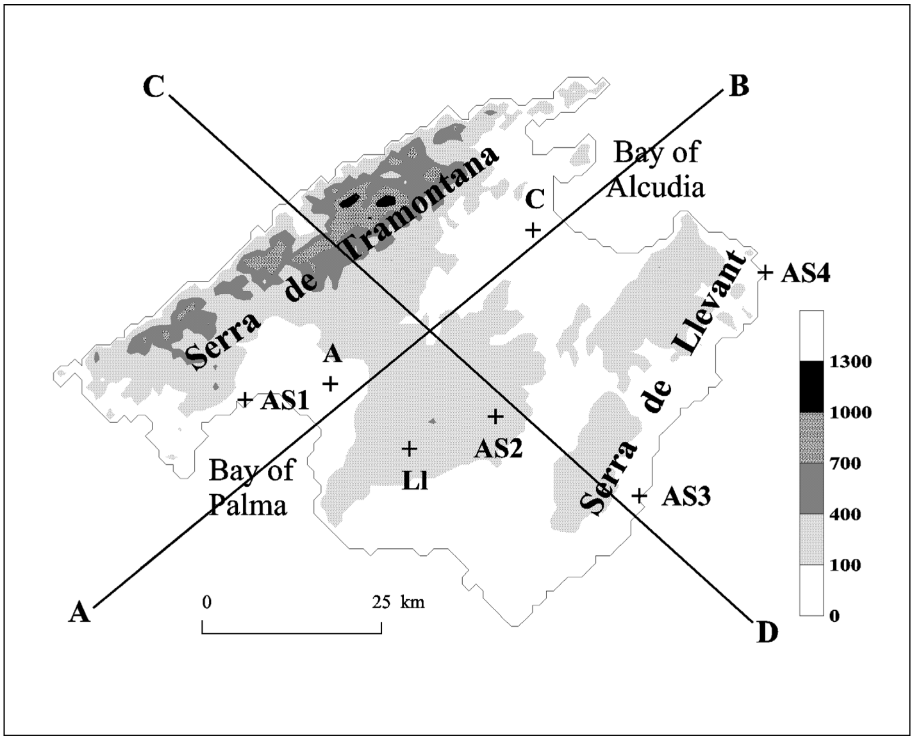

Figure 1: The island of Mallorca. Orography and the sites refered in the text are indicated. ASn represent the location of the automatic weather stations, A represents the airport observatory, C the climatological station and Ll the town of Llucmajor. AB and CD indicate the cross-sections analysed in the text.

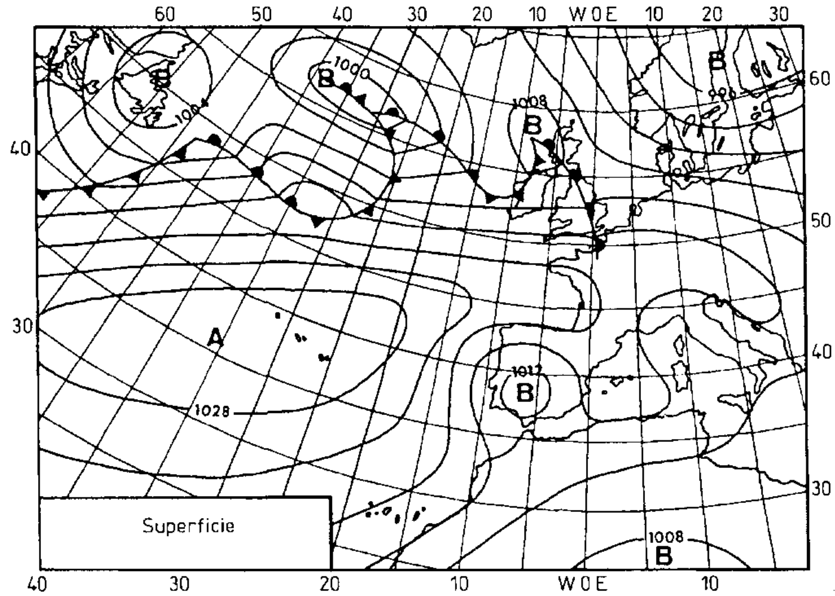

Figure 2: Typical synoptic situation during summer in central and western Europe. A and B represent high and low pressure respectively. (after Font 1983).

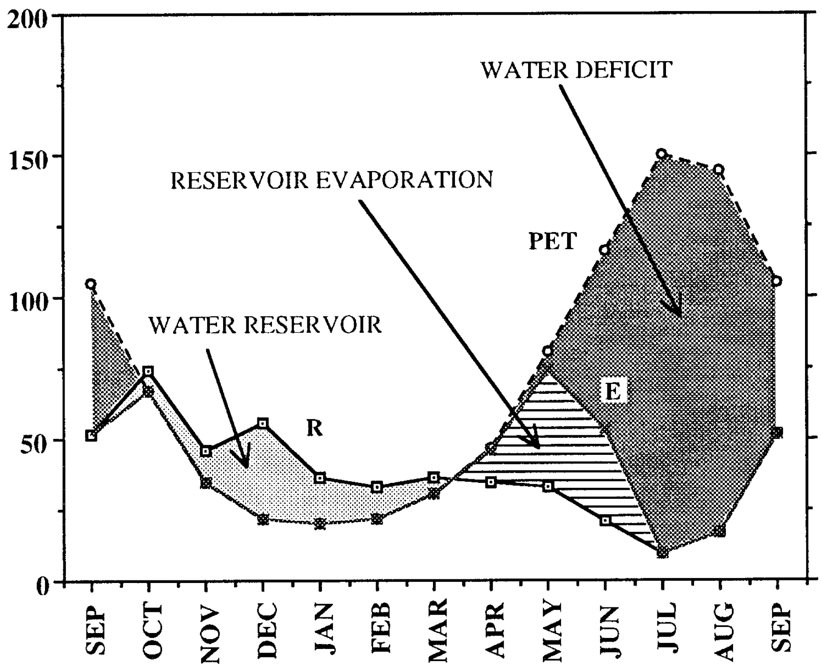

Figure 3: Thornthwaite climatologic hydric balance in Llucmajor (see Fig. 1 for location). R=rainfall, E=evaporation, PET= potential evapotranspiration.

(a)

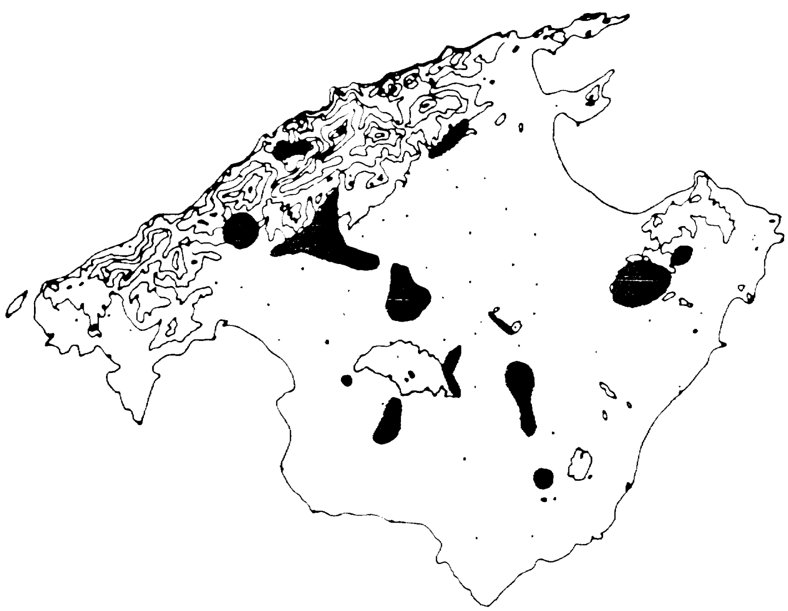

(b)

Figure 4: (a) Streamlines of the mature sea breeze in Mallorca, and (b) Convergence zones (after Jansà and Jaume, 1946); reproduced by permission of Rev. de Geofísica).

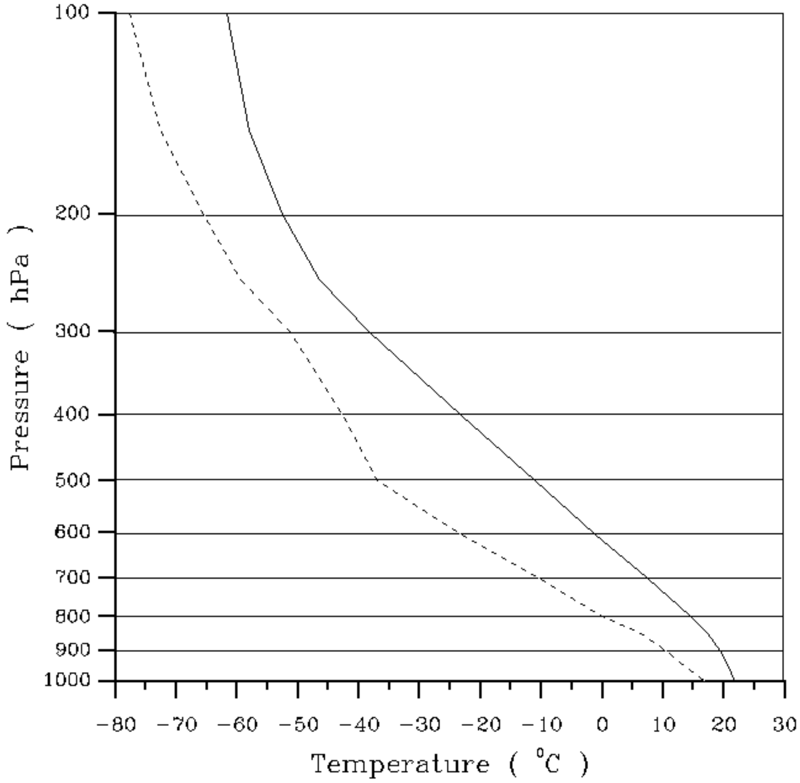

Figure 5: Mean vertical structure of the atmosphere over Mallorca for July at 0000 UTC (after Ramis, 1976). Solid line represents temperature and dashed line represents dew point.

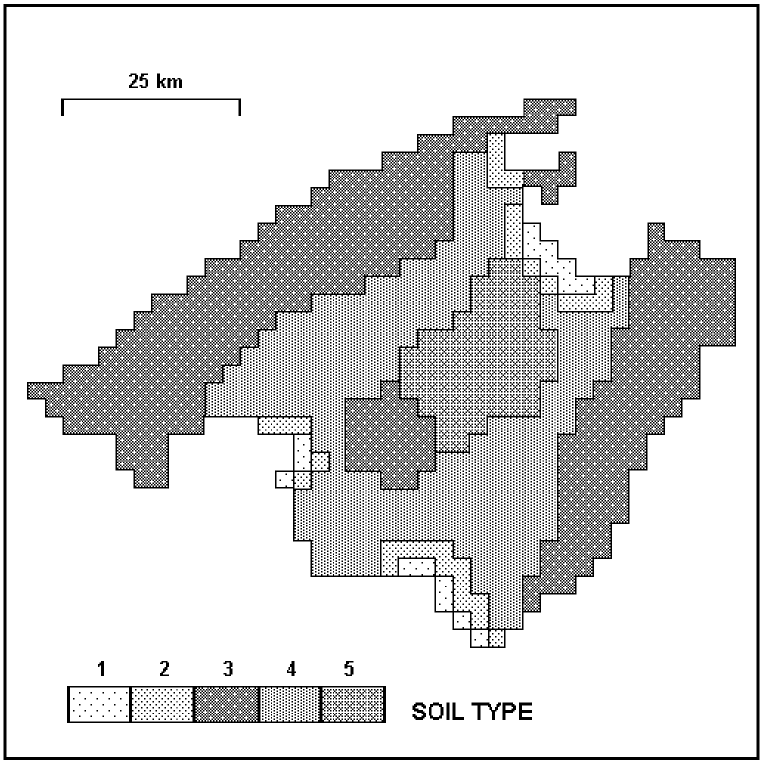

(a)

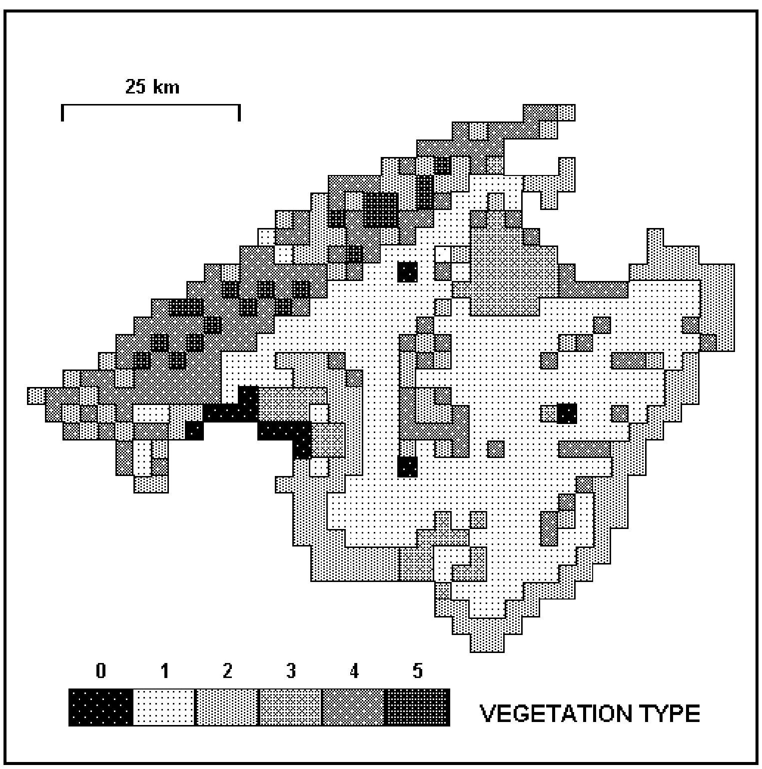

(b)

Figure 6: (a) Soil distribution on Mallorca: 1=sand, 2=sandy loam, 3=silt loam, 4=clay loam and 5=clay; (b) Vegetation distribution: 0=bare, 1=grass, 2=shrub, 3=crop, 4=forest and 5=woodland; (c) Shielding factor; (d) Regional multiplicative factor used to compute the soil moisture on the island.

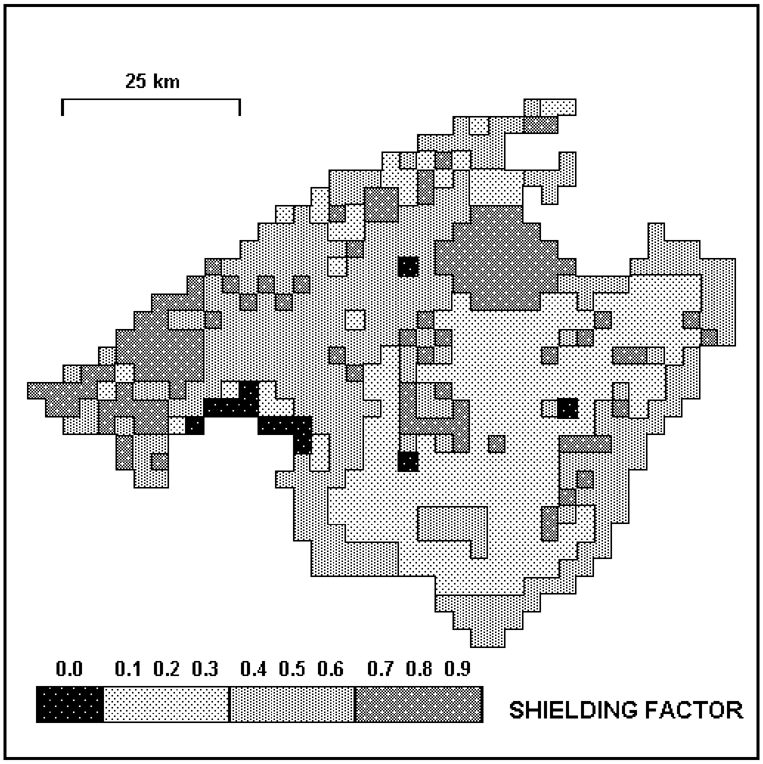

(c)

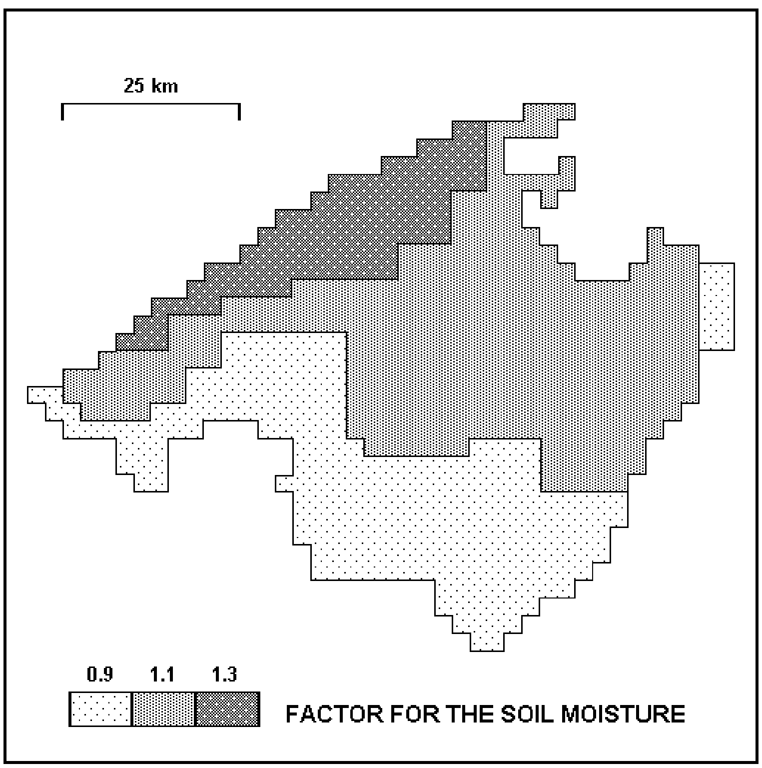

(d)

Figure 6 (cont.).

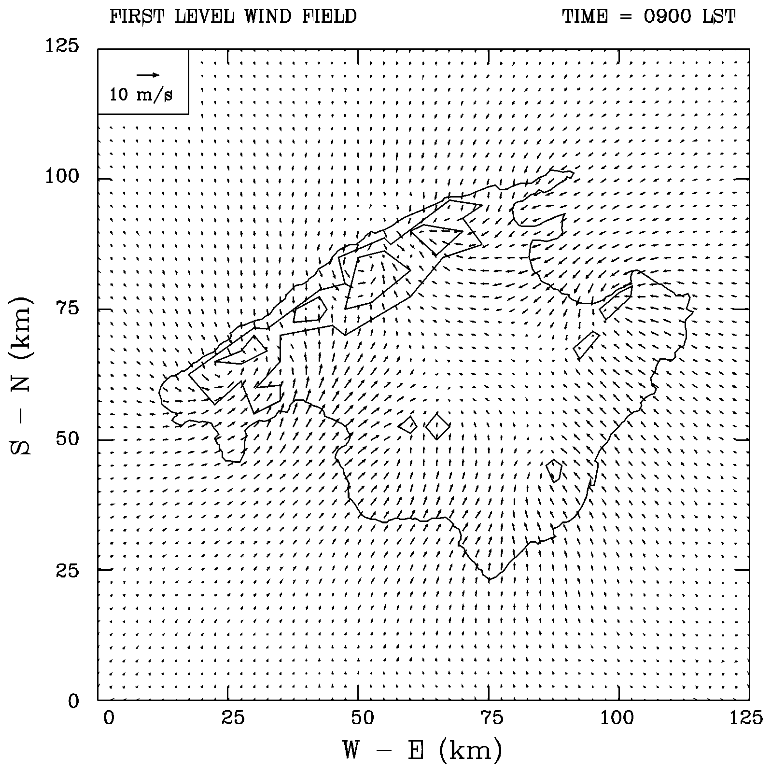

(a)

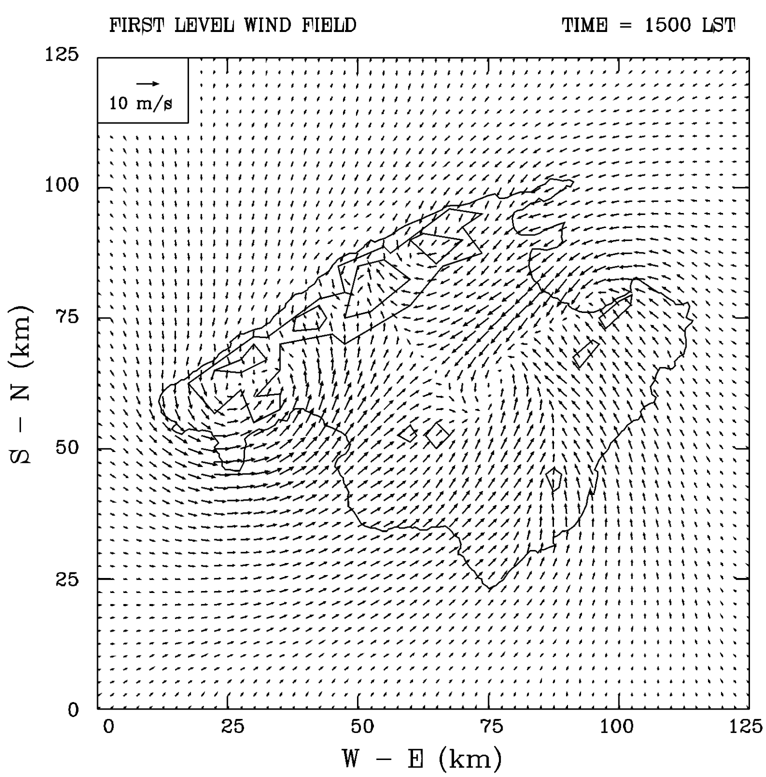

(b)

Figure 7: Diurnal evolution of the sea breeze. (a) 0900 LST; (b) 1500 LST; (c) 2100 LST and (d) 0500 LST. The arrow on the upper left corner represents 10 $\mathrm{m\,s^{-1}}$. Orographic contours of 300 and 700 m are included.

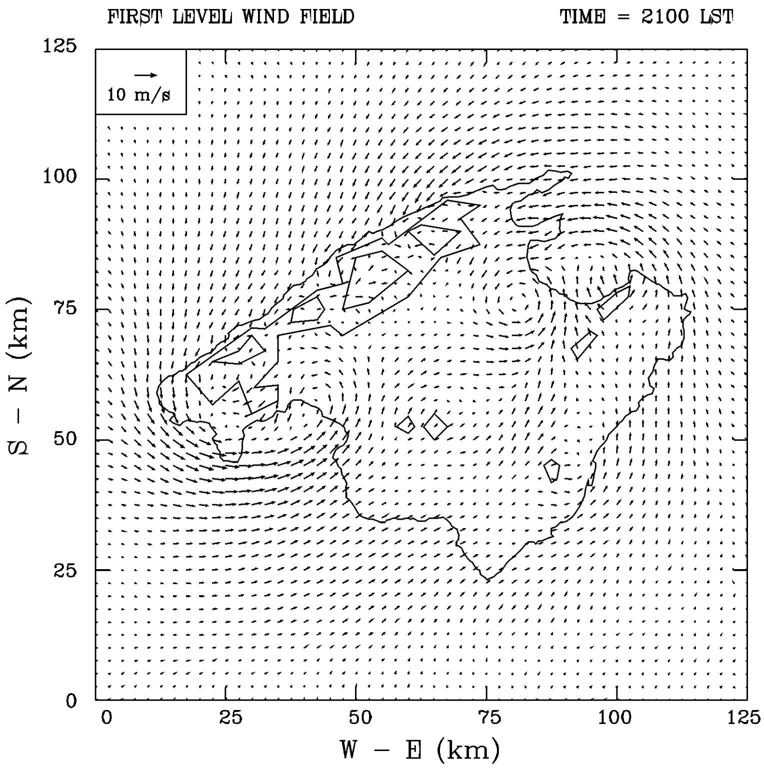

(c)

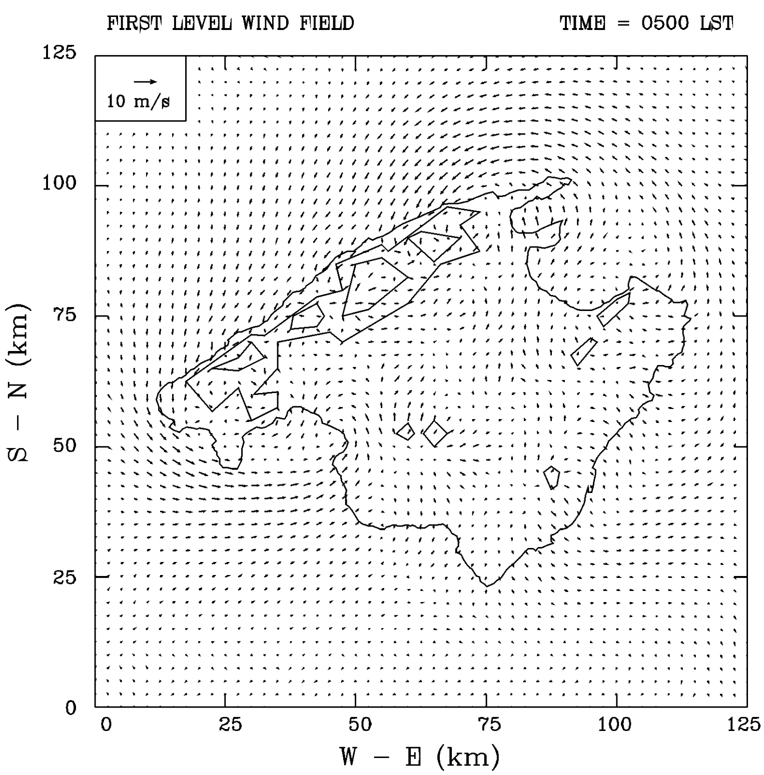

(d)

Figure 7 (cont.).

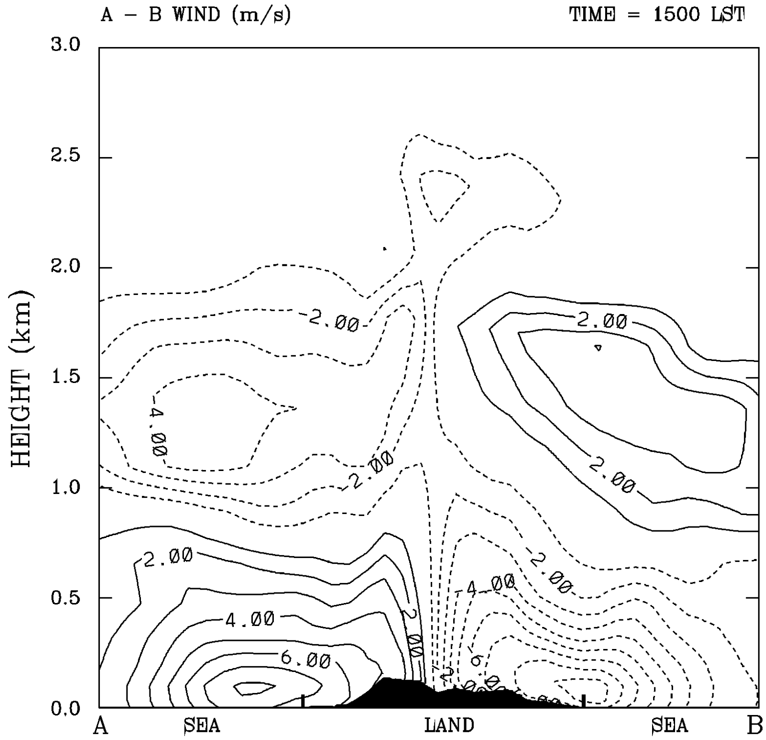

(a)

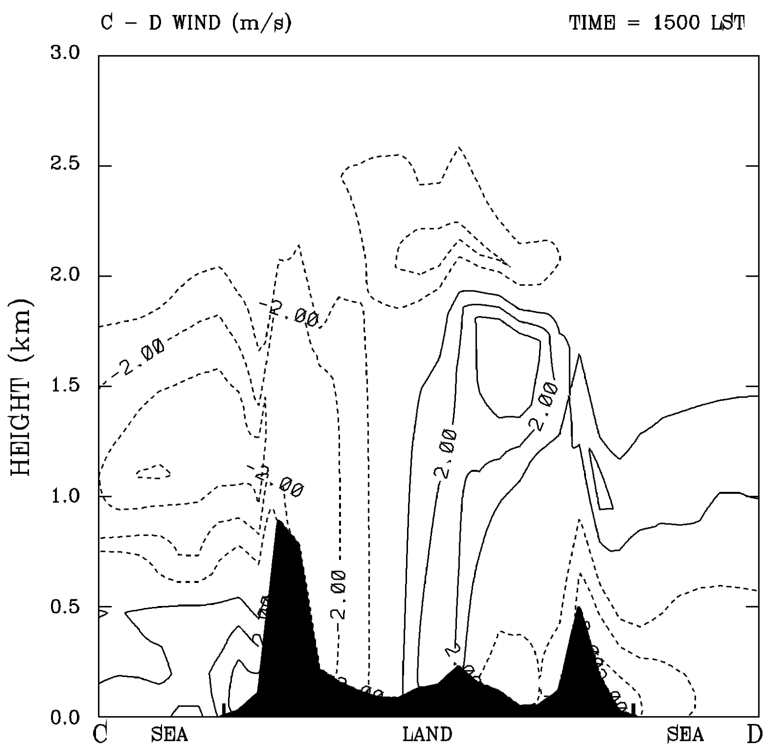

(b)

Figure 8: Vertical cross section showing the horizontal wind component ($m\,s^{-1}$) at 1500 LST: (a) along AB (positive values, in solid line, are from the southwest); (b) along CD (positive values from the northwest). Contour interval is 1 $m\,s^{-1}$ and zero contour is not shown.

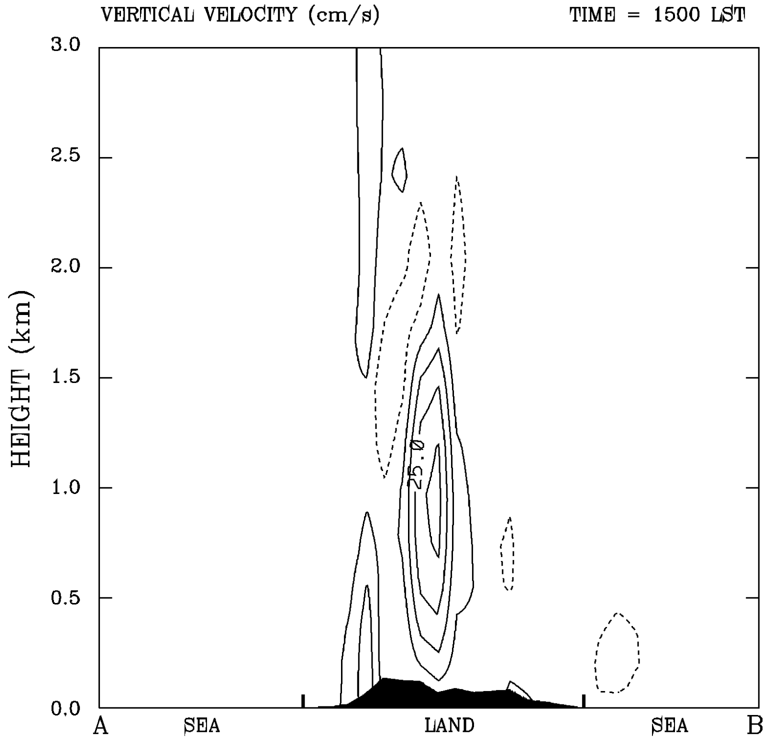

Figure 9: Vertical cross section along AB showing the vertical velocity field ($\mathrm{cm\,s^{-1}}$) at 1500 LST. Contour interval is 10 $\mathrm{cm\,s^{-1}}$ starting at 5 $\mathrm{cm\,s^{-1}}$ for solid contour (ascending motion) and -5 $\mathrm{cm\,s^{-1}}$ for dashed contour (descending motion).

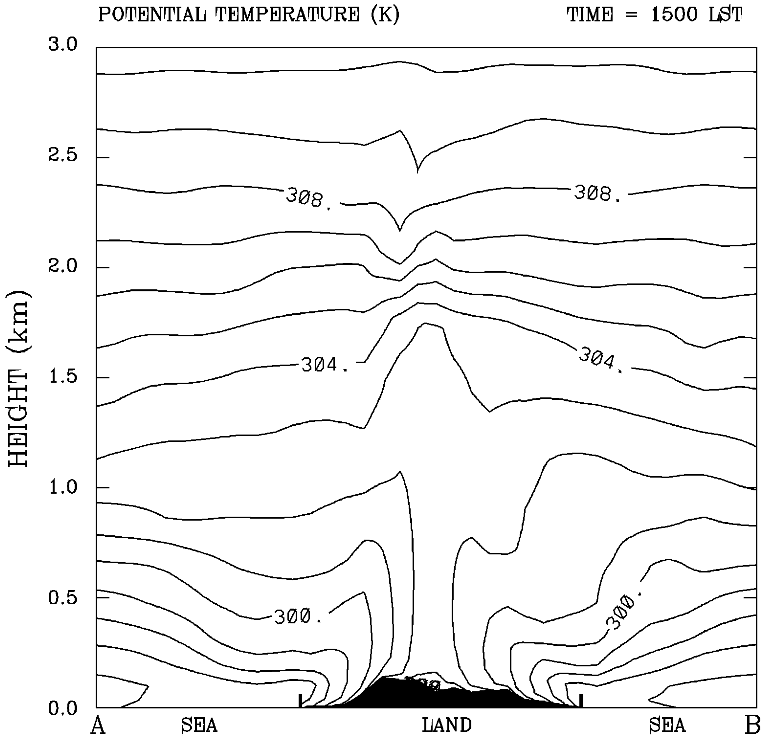

Figure 10: Vertical cross section along AB showing the potential temperature (K) at 1500 LST. Contour interval is 1 K.

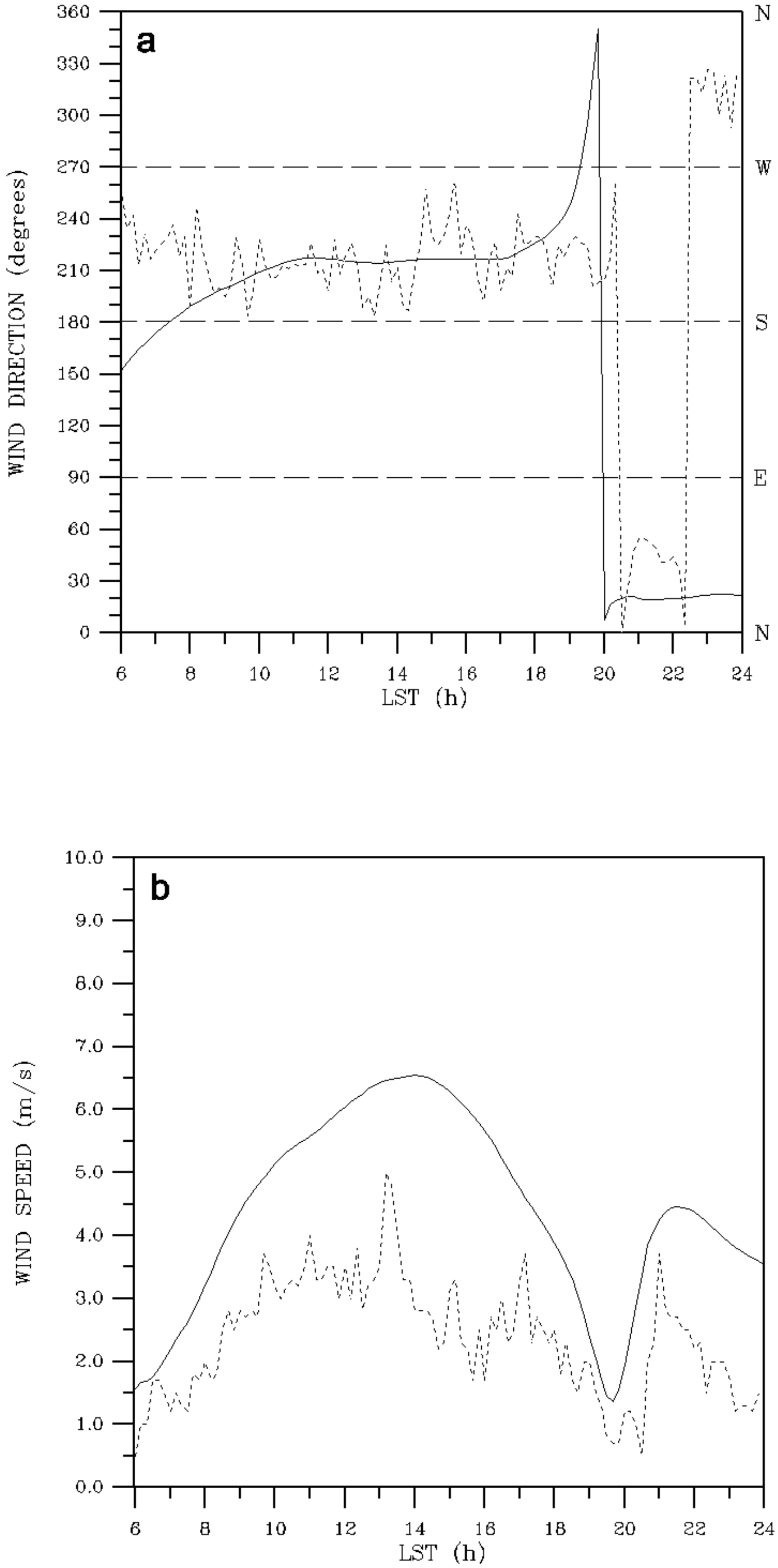

Figure 11: Model results (solid line) compared against observations on 22 July 1993 (dots) in AS1: (a) wind direction; (b) wind speed; (c) temperature and (d) relative humidity.

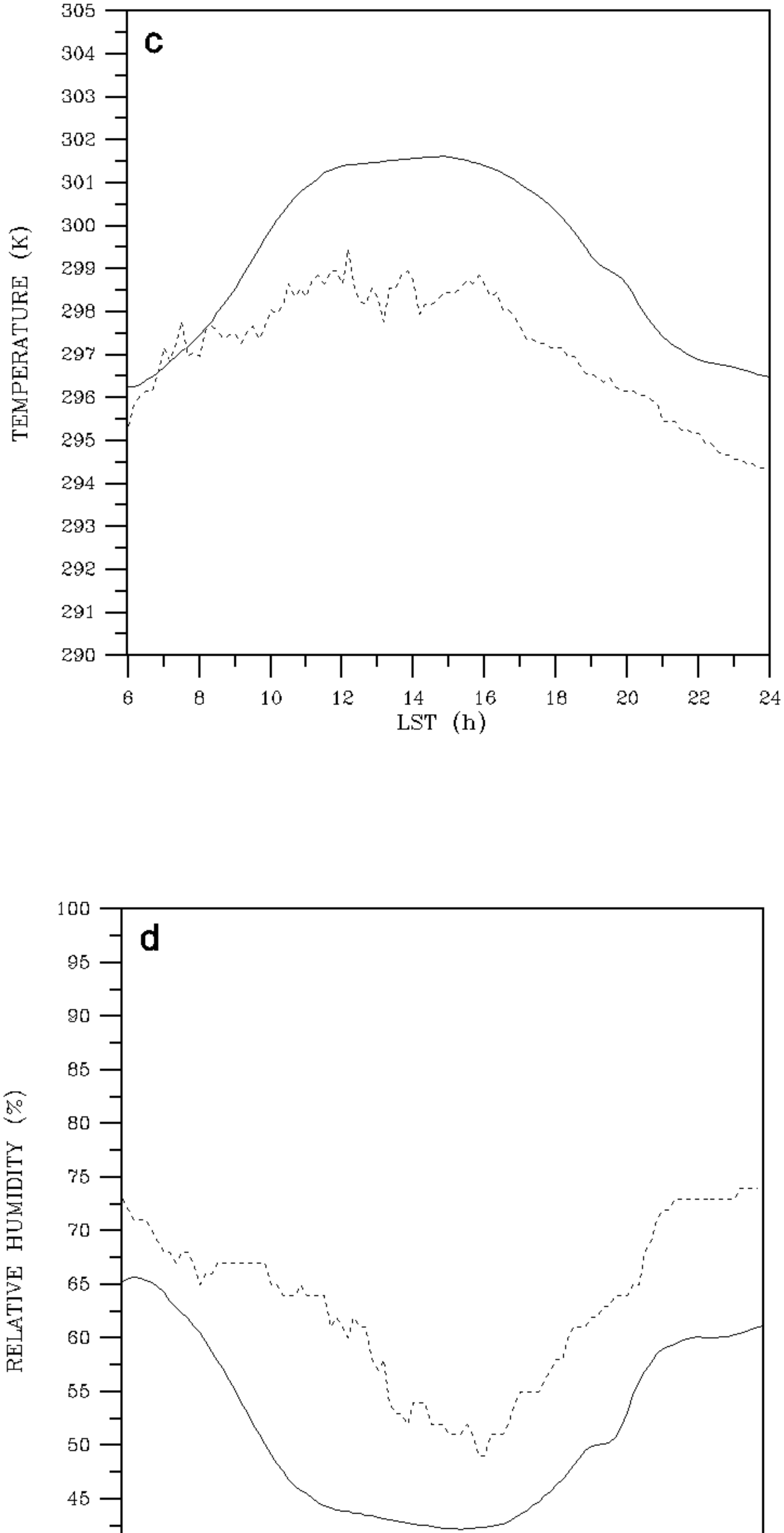

Figure 11 (cont.).

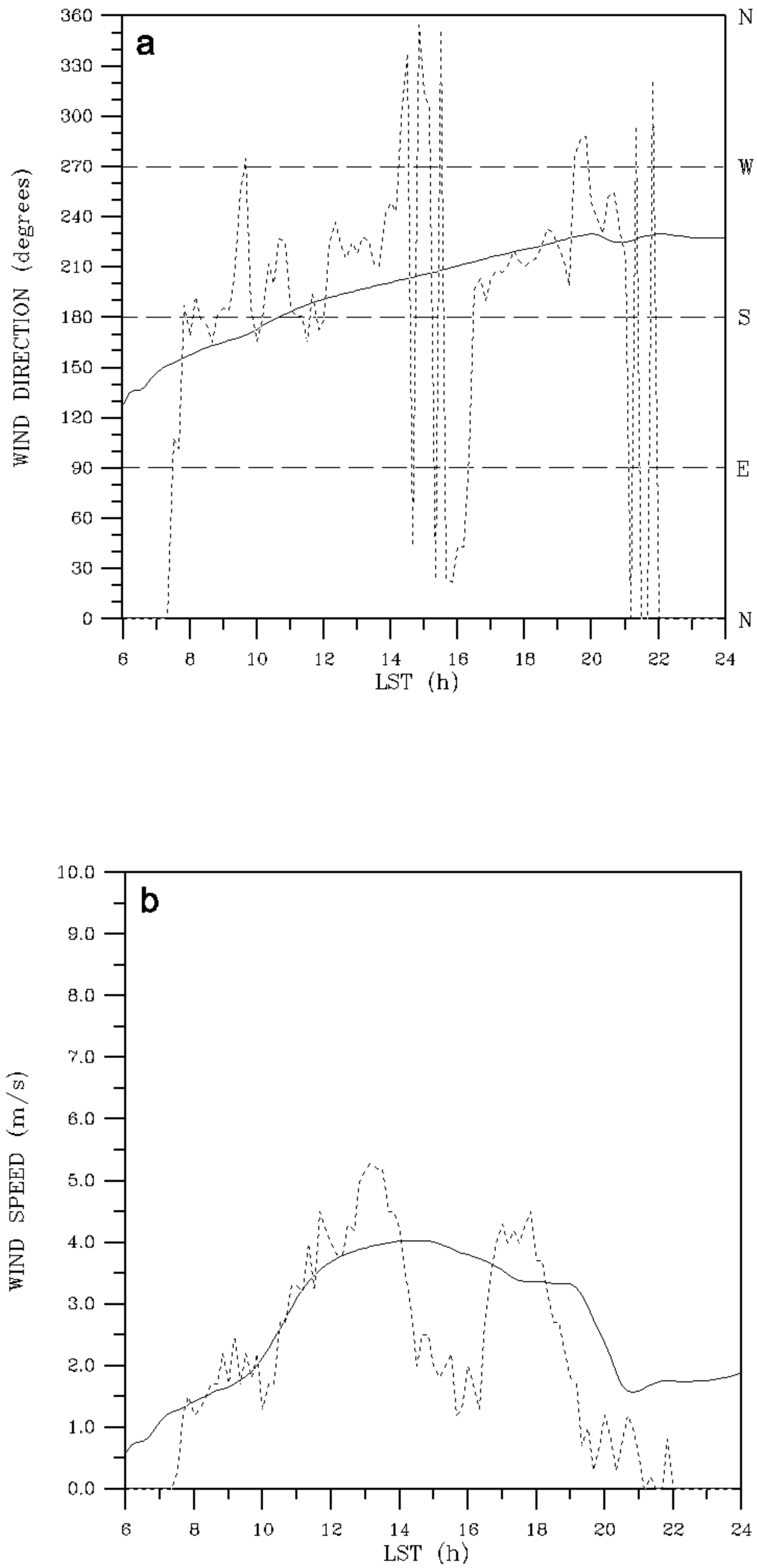

Figure 12: The same as in Fig. 11 but in AS2 for: (a) wind direction; (b) wind speed.

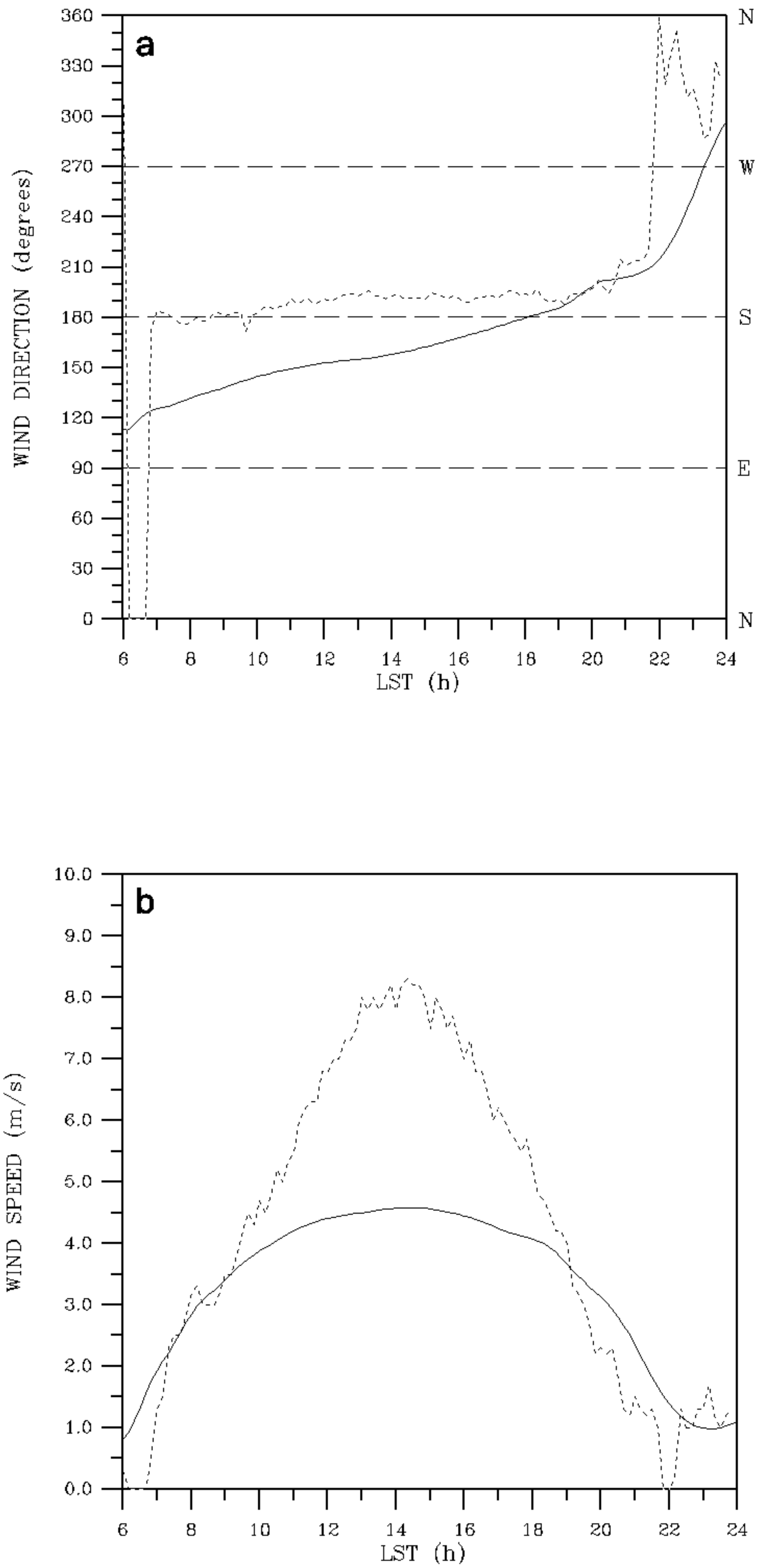

Figure 13: The same as in Fig. 11 but in AS3 for: (a) wind direction; (b) wind speed.

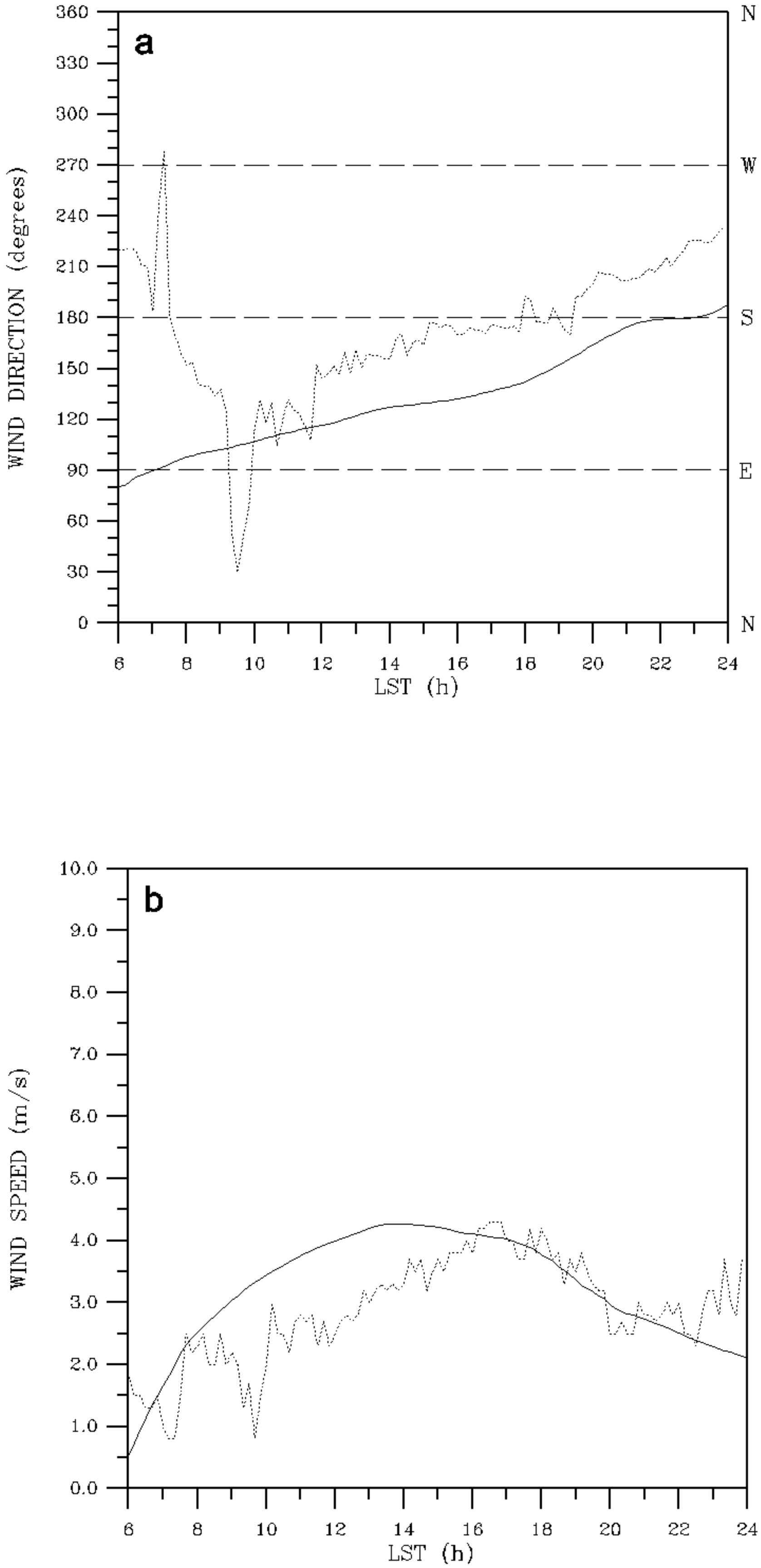

Figure 14: The same as in Fig. 11 but in AS4 for: (a) wind direction; (b) wind speed.

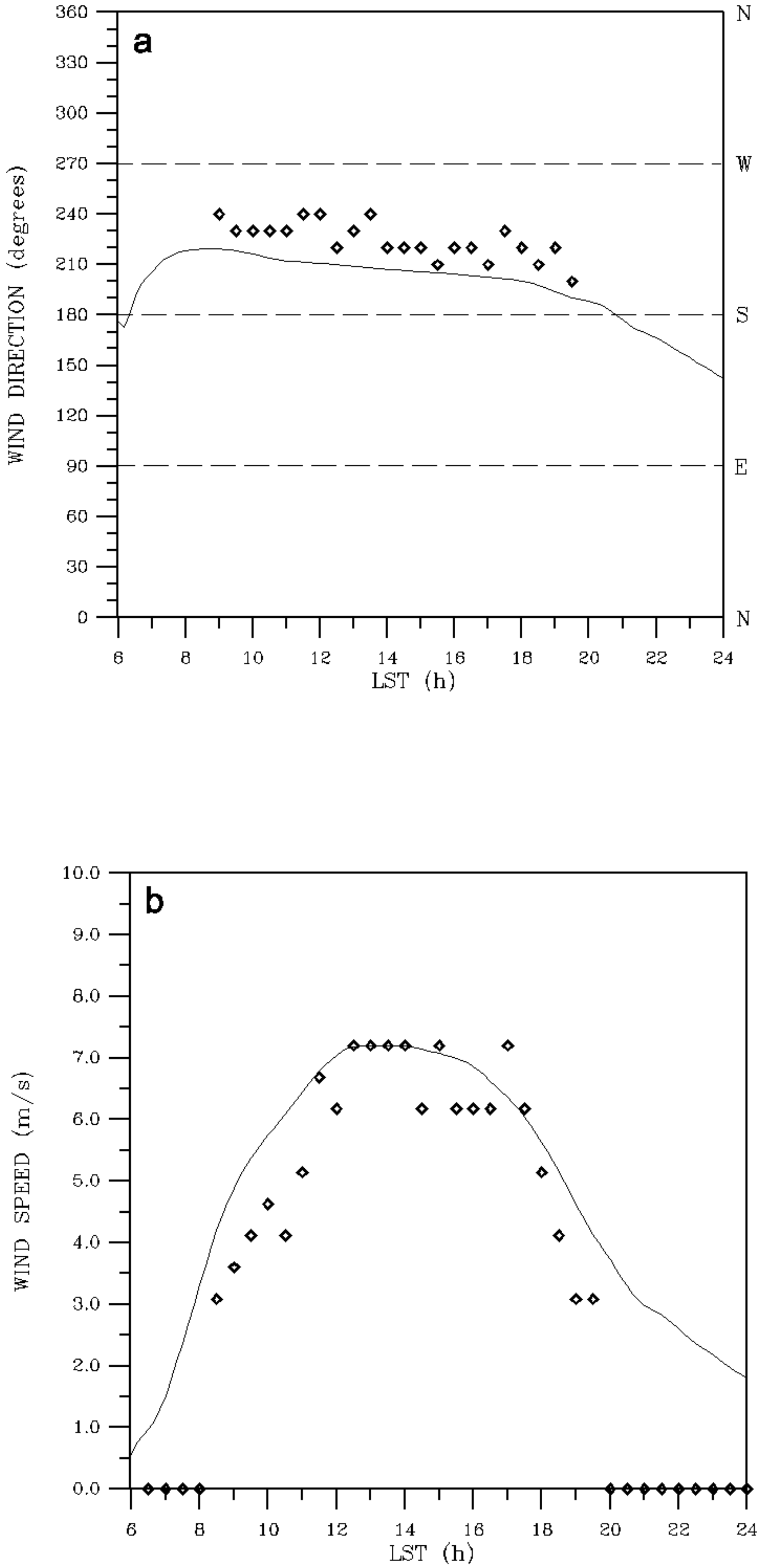

Figure 15: Model results (solid line) against observations on 22 July 1993 (rhombs) in A: (a) wind direction; b) wind speed.

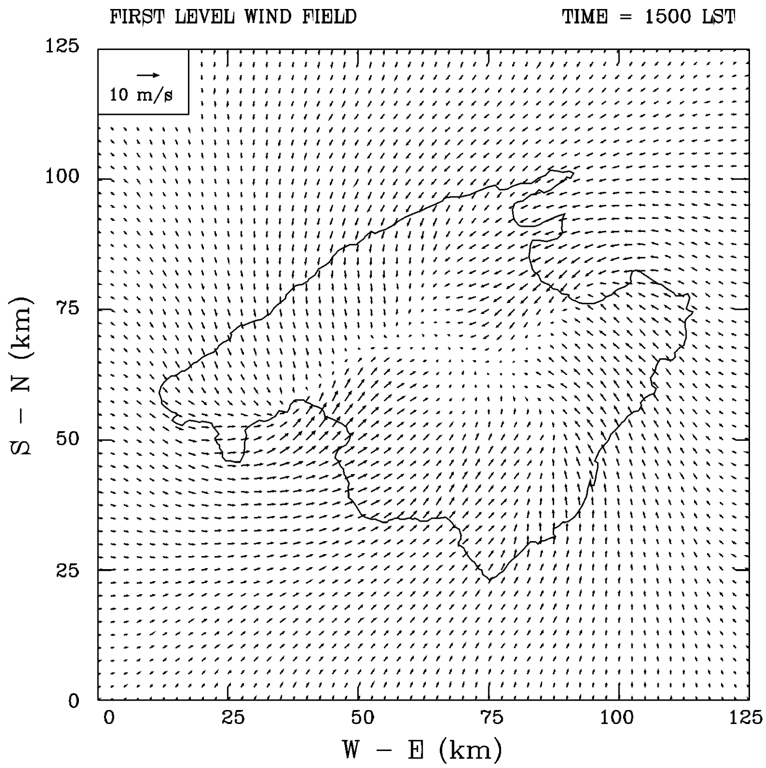

(a)

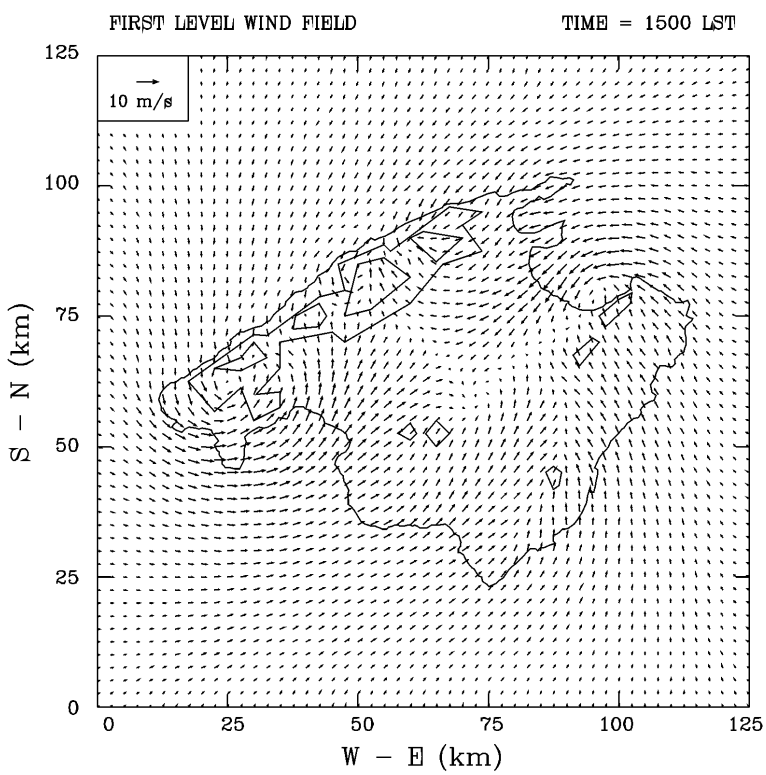

(b)

Figure 16: Results at 1500 LST for the experiments: (a) without orography and with saturated soil; (b) with orography and saturated soil; (c) without orography and with dry soil.

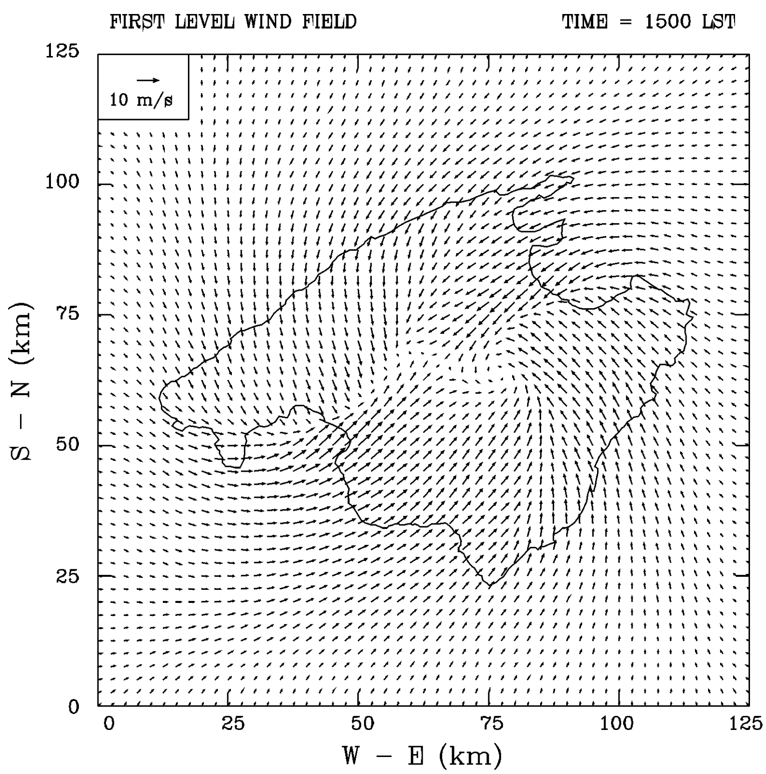

(c)

Figure 16 (cont.).

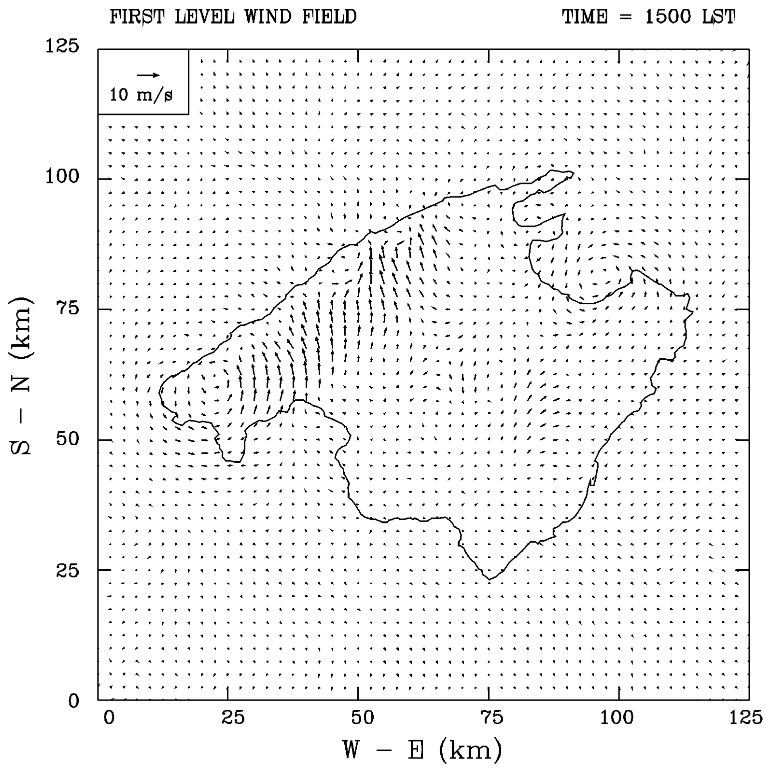

(a)

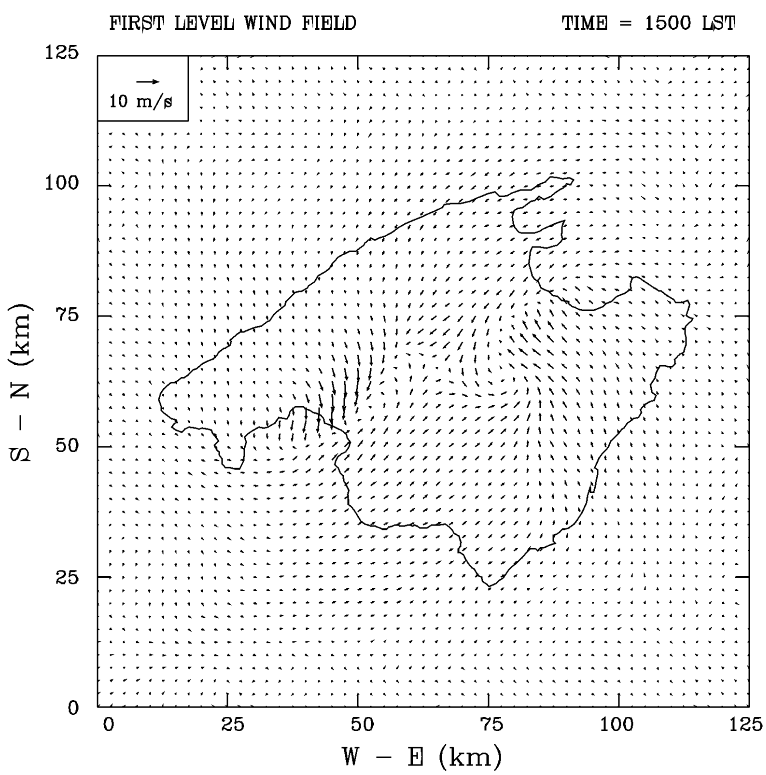

(b)

Figure 17: Effects on the sea breeze circulation at 1500 LST by the factors: (a) orography; (b) soil dryness; (c) interaction between orography and soil dryness.

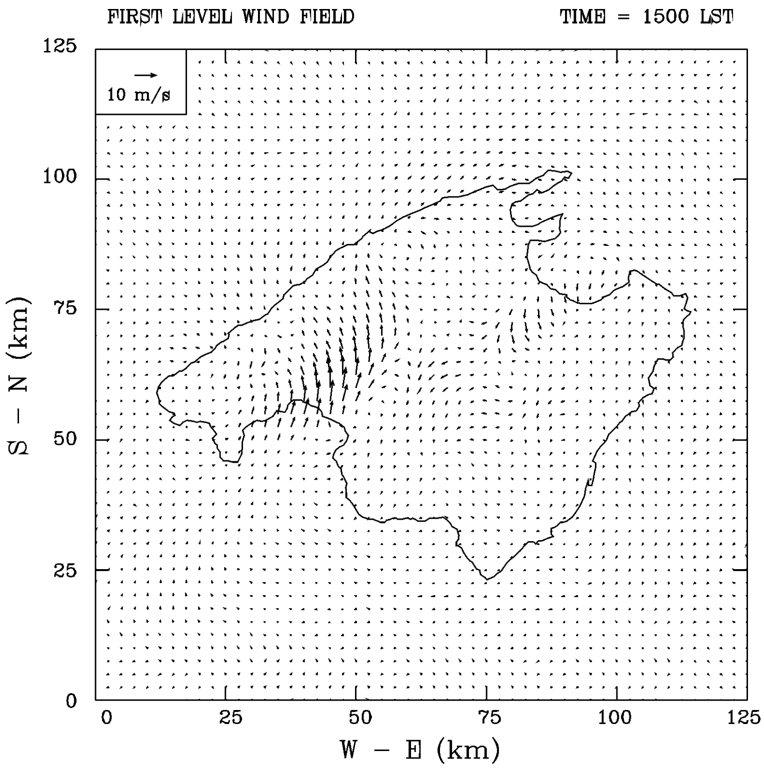

(c)

Figure 17 (cont.).